PHOTOMETRY OF THE MARTIAN ATMOSPHERE: AN IMPROVED PRACTICAL MODEL FOR CARTOGRAPHY AND PHOTOCLINOMETRY. R. L. Kirk, K. T. Thompson, and E. M. Lee[1], [1]U.S. Geological Survey, 2255 N. Gemini Dr., Flagstaff, AZ 86001 (rkirk@usgs.gov).

Introduction: This abstract describes recent work on approximate modeling of radiative transfer in the martian atmosphere with applications to the photometric normalization of images for cartographic products and for quantifying and improving the accuracy of topographic models obtained by photoclinometry, also known as shape-from-shading.

One year ago, we described [1] a major effort to improve the photometric modeling and correction software in the USGS Integrated Software for Imagers and Spectrometers (ISIS) system. Motivated by the desire to make photometrically corrected image mosaics of Mars [2, 3] and the Galilean satellites [4, 5], we created a greatly enhanced new program called PHOTOMET to do photometric normalization of images in which we

- greatly increased the variety of surface scattering models
- implemented more realistic yet reasonably efficient models of atmospheric scattering
- allowed normalization of albedo variations, topographic shading, or a mixture (i.e., normalization of albedo at low incidence angles blending smoothly to normalization of topography near the terminator)
- modularized the software so photometric functions, atmospheric scattering models, and normalization options could be combined freely

In addition, we provided a tool called SHADOW_TAU for estimating the atmospheric optical depth in an image from the calibrated reflectance values of a shadow and of a nearby level region. The normal albedo of the shadow and level areas is assumed to be the same and is estimated simultaneously with optical depth. The results are model-dependent, but SHADOW_TAU uses the same model as PHOTOMET so, the estimated optical depth is appropriate for use in the latter program.

On the whole, our new software yielded substantial improvements in the photometric normalization of images of airless bodies [5] but the results for Mars, on which atmospheric scattering of light contributes significantly to the images, were less successful. The albedo and optical depth values we obtained from shadow measurements appeared reasonable individually, but examination of the results for several hundred Viking Orbiter images covering the entire planet revealed that albedo and optical depth were each correlated with both the incidence and phase angles [1]. Applying the software (and optical depth values) to normalize the images of the global mosaic made it plain that this was not the result of a sampling effect, but was caused by a shortcoming in the models. Adjacent images with different illumination (in particular, with large or small versus intermediate phase angles) did not match in brightness and contrast after normalization. To produce a cosmetically acceptable mosaic, we resorted to a least-squares adjustment of brightness and contrast of each image sequence to minimize variations between sequences [2].

An obvious candidate for the weakness of our atmospheric model was its failure to take into account the extremely forward-scattering character of martian atmospheric particles [6, 7, 8]. The analytic scattering model, which is described below, has been developed only for isotropic and weakly anisotropic (one-term Legendre polynomial for the single-particle phase function) scattering. As we pointed out [1], forward scattering would result in increased scattering onto the surface at low phase angles and increased scattering to the camera at large phase angles, corresponding to what our model interprets as larger albedos in these situations. We have therefore extended the analytic model by adding an approximate correction for arbitrary phase function in the singly scattered light only.

Analytic Atmospheric Scattering Model: Our models attempt to balance the need for a relatively simple, fast calculation of the additive and multiplicative effects of atmospheric scattering with the desire for physical realism. We use Chandrasekhar's [9] solution of the "planetary problem" of a slab atmosphere over a reflective surface (§72). The derivation strictly applies only to a Lambert surface because it takes account of the fraction of incident photons reflected from the surface but not their angular distribution. We therefore approximate the actual surface photometric model by numerically calculating the albedo of an "equivalent Lambert model." For the term involving surface illumination of sunlight, we use the hemispheric albedo A_h, which is averaged over emission angle, whereas for surface illumination by light from the atmosphere we use the bihemispheric albedo A_b, which is averaged over both incidence and emission angles. In addition, we correct the overall result by assuming that the light that passes through atmosphere completely unscattered is reflected according to the detailed surface photometric model rather than by Lambert's (We do not apply the detailed surface law to light scattered in the atmosphere before hitting the surface; this would require calculation of and averaging over the detailed angular distribution of sky light, which would be prohibitively slow. This effect will be unimportant if the surface is nearly Lambertian or if the sky light is only weakly directional.) Our atmospheric scattering model can be written in the form

$$p(\mu_0,\mu,\alpha) = p_{std}(\mu_0,\mu,\alpha) + \frac{\rho A_h(\mu_0)\mu_0 T(\mu_0,\mu,\alpha)}{1-\rho\bar{s}A_b} + T_0(\mu_0,\mu,\alpha)\rho\left(p_{surf}(\mu_0',\mu',\alpha) - A_h(\mu_0)\mu_0\right)$$

where we use the symbol p for photometric functions (p_{std} is the solution to the "standard" problem of an atmospheric layer with no surface scattering, [9], Chapter IX), μ_0 and μ are cosines of the incidence and emission angles for a level surface and μ_0' and μ' are those including local topography, α is the phase angle, and ρ is a factor by which the local albedo departs from our model. Because the equation is nonlinear in ρ, we must explicitly include this variable and solve for it to do albedo normalization, rather than simply dividing the image by the model. The atmospheric contribution p_{std}, overall two-way transmission T, two-way unscattered transmission T_0, and s, which measures the total fraction of light scattered from sky to land, can all be evaluated in terms of Chandrasekhar's functions X and Y ([9], Chapter VIII). We evaluate X and Y by using the first- and second-order expansions in the normal optical depth τ given in §63 and §65. These expansions are worked out, giving all required quantities in closed form, for the cases of isotropic scattering and scattering according to the one-term Legendre phase function $1+x\cos(\Theta)$. The remaining parameters are the asymmetry parameter x and the single-scattering albedo ω_0.

Correction for Anisotropic Scattering: The maximum anisotropy described by the analytic model, with x=-1, is weak: the phase function varies linearly from 1 in the forward direction to 0 in the backward direction so the "forward scattering lobe" is 90° wide, and the anisotropy parameter $\langle\cos(\Theta)\rangle$ is only 1/3. Observations of the martian atmosphere indicate that the forward scattering lobe is much narrower and stronger than this, with $\langle\cos(\Theta)\rangle$=0.67 to 0.77 [6, 7, 8]. A practical solution is to add to the analytic scattering results for isotropic scatterers a correction for singly scattered light with an arbitrary phase function. This approach is familiar in a planetary context because it was used by Hapke [10] to model surface scattering. To apply it to atmospheric scattering, we simply need to make the corresponding correction to the formulae for a slab of finite optical depth rather than a half space. The singly scattered contributions to reflection and transmission of the atmosphere are given in [9], p. 217. So, for example, the correction to the upward scattering term p_{std} is $\omega_0\mu_0/4(\mu_0+\mu)\,(p(\Theta)-1)\,(1-\exp(-\tau\,(1/\mu_0+1/\mu)))$. Corrections to the other quantities of interest, s, T, and T_0, are obtained as multiple integrals over this and the corresponding expression for atmospheric transmission. For the single-scattering phase function $p(\Theta)$ we adopt a single-term Henyey-Greenstein function [11], which fits the inferred phase function of martian aerosols [7, 8] quite well. Unfortunately, the needed integrals over this function must be evaluated numerically.

Shading and shadowing. The directionality of the singly scattered light in our revised model requires us to rethink the evaluation of both the transmission factor T_0 relevant to topographic shading and the evaluation of shadow intensities. In our previous model we assumed that it is the never-scattered light that contributes to shading and whose absence defines a shadow (i.e., that a shadow is hidden from the sun but "sees" the entire sky). With a more realistic forward-scattering atmosphere, these approximations are no longer adequate. To evaluate the downward transmission factor in T_0 we calculate the horizontal component of flux, both transmitted and scattered, at the bottom of the atmosphere, and scale it to that at the top. This horizontal component determines how the flux varies on a sloping surface, which is the sole determinant of the surface brightness for a Lambert scatterer and should be a reasonable approximation even in the non-Lambertian case. For the upward transmission factor we include only the unscattered light, on the assumption that even the singly scattered light from the surface will blur adjacent topographic features and hence not contribute to shading.

The definition of a "shadow" when the sky illumination is diffuse yet highly directional is problematic. Clearly, the brightness of a region hidden from the sun depends on how much of the sky it sees and there is no one value of shadow intensity as in the atmosphere-free case. (This is true also for an isotropically scattering atmosphere, but the effect is much weaker because the sky brightness is uniform). As a simple yet reasonable choice, we model shadows as being illuminated only by the half of the sky opposite the sun.

Estimation of Optical Depth & Application to Cartography: Application of the new model, with Henyey-Greenstein parameter g=0.7, to our previous shadow measurements considerably improves the believability of the results. The apparent correlations of optical depth and albedo with incidence angle are eliminated and the correlations with phase angle are greatly reduced. There is still a suggestion of lower optical depths near 90° phase but we are satisfied that this is a sampling effect, as these observations come from a very restricted time period when the optical depth is known to be small [12]. There is also a tendency for albedos to increase at phase angles from 105° to 130° (the maximum observed). This may be a shortcoming in our surface scattering model rather than in the atmospheric model. We use a Hapke surface model with parameters estimated from Mars Pathfinder observations of Mermaid [13] except for the macroscopic roughness [1]. Mermaid showed no evidence of a forward-scattering lobe whereas other materials at the Pathfinder site did [13] and so might the average Mars.

We compared our optical depth estimates with the maps of 9-µm opacity compiled from IRTM measurements [12]. IRTM observations were available at the same time, latitude, and longitude for only about 25% of our shadows; for the remainder, we compared the zonal average of data from [12] at the same time and latitude. The results are consistent with past comparisons of visible and IRTM opacity [14]: our optical depths are almost never less than 2 times the 9-µm value and are sometimes as much as 0.5 units greater. The latter difference may reflect a component of aerosols that are too fine to contribute to 9-µm opacity.

The final test of the new model is its use to normalize images intended for mosaicking. Brightness and contrast variations between normalized images with different illumination are substantially reduced compared to the older model, as we will show in our poster.

Implications for Photoclinometry: Our ability to model the brightness and the contrast of topographic shading for a surface seen through an atmosphere at given geometry and optical depth provides useful insights into the accuracy of, and limitations on, photoclinometric techniques for Mars. For example, Figure 1 illustrates the reduction of topographic contrast by atmospheric opacity as a function of incidence angle (with emission angle zero). The contrast for small slopes is plotted on an inverse scale, as the slope that would be required to give 1% contrast (roughly the minimum visible). The existence of a "point of diminishing returns" beyond which increasing the incidence angle no longer improves the contrast is the most interesting feature of this plot.

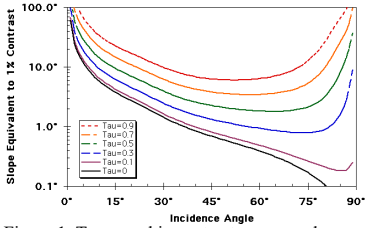

Figure 1. Topographic contrast, expressed as slope having 1% contrast, vs. incidence angle and optical depth tau.

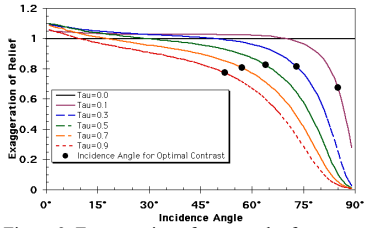

Figure 2. Exaggeration of topography from photoclinometry on images after subtraction of shadow intensity.

We can also use our photometric model to evaluate an important aspect of the accuracy of photoclinometry, namely the suitability of the usual correction for atmospheric scattered light. The most common approach for carrying out photoclinometry with both 1D [15] and 2D [16] approaches is to identify a shadow and subtract its measured intensity from the whole image. After subtraction of this "haze" value, the remaining multiplicative effect of the atmosphere on intensity is lumped with the (unknown) surface albedo and the combination of the two factors is adjusted to make all or part of the topographic surface level. Our model predicts, however, that the transmission factors for the mean brightness, for infinitesimal slopes, and for shadows are not all the same. Figure 2 shows the ratio of the topography that will be obtained by photoclinometry on images normalized as described to the actual topography. Considering that small incidence angles are not suitable for photoclinometry, we see that the result is always an underestimate of the relief. In essence, subtracting a very dark shadow lit by only half the sky undercorrects the images. Nevertheless, if the incidence angle is limited to less than the "point of diminishing return" then the error in the scale of the topography is no more than about 20%. This is comparable with other error sources that have been considered [17].

A promising alternative to correcting images for photoclinometry by subtraction of the shadow intensity is the adjustment of an atmospheric model (whether a detailed model such as we have described or a simple additive/multiplicative correction) to give results consistent with an independent estimate of the topography. The increasing density of MOLA altimetric data makes this a viable approach. A companion abstract [18] describes our adjustment of the additive and multiplicative normaliztion of MOC images to fit slopes reported by MOLA. We were forced to compare slopes over long (multi-kilometer) baselines because, until recently, it has not been possible to coregister MOC and MOLA datasets to high precision. With the availability of refined pointing angles for the two instruments that yield coregistration to <100 m [19] it will be possible to make detailed comparisons between altimetry and photoclinometry. The result will be not only to increase the accuracy of photoclinometric topography (and extend and densify the MOLA measurements) but also to determine the atmospheric opacity and even to test the adequacy of surface and atmospheric photometric models.

References: [1] Kirk, R. L., et al. (2000) *LPS XXXI,* 2025. [2] Kirk, R. L., et al. (2000) *LPS XXXI,* 2011. [3] Kirk, R. L., this conference. [4] Becker, T. L., et al. (1999), LPS XXX, 1692. [5] Becker, T., et al., this conference. [6] Pollack, J. B., et al., 1995, *J. Geophys. Res., 100,* 5235. [7] Tomasko, M. G., et al., 1999, *J. Geophys. Res., 104*, 8987. [8] Markiewicz, W. J., et al., 1999, *J. Geophys. Res., 104*, 9009. [9] Chandrasekhar, S., 1960, *Radiative Transfer*, Dover, 393 pp. [10] Hapke B., 1981, *J. Geophys. Res., 86,* 3039. [11] Henyey. L. G., and J. L. Greenstein, 1941, *Astrophys. J., 93,* 70. [12] Martin, T. Z., and Richardson, M. I., 1993, *J. Geophys. Res., 98,* 10,941. [13] Johnson, J. R., et al., 1999, *J. Geophys. Res., 104,* 8809. [14] Clancy, T. R., et al., 1995, *J. Geophys. Res., 100*, 5251. [15] Davis, P. A., and L. A. Soderblom, 1984, J. Geophys. Res., 89, 9449. [16] Kirk, R. L., 1987, *A fast finite-element algorithm for two-dimensional photoclinometry*, III, Ph.D. Thesis, (unpubl.), Caltech. [17] Jankowski, D. G., and S. W. Squyres, 1991, *J. Geophys. Res., 96*, 20,907. [18] Herkenhoff, K. E., and R. L. Kirk, this conference. [19] Kirk, R. L., et al., this conference.